T. P. Sanfirova, and A. F. Ioffe, Preprint of the International Symposium on Macromolecules, Helsinki, Finland, Jul 2-7, 1972, Vol. 5, 163.
(28) In that new representation, the stochastic process still visits primary bonds with the same probability as secondary bonds, since one must not overlook the fact that each node itself actually represents m primary bonds aligned in series along the y axis.
(29) D. L. M. Cansfield, I. M. Ward, D. W. Woods, A. Buckley, J. M. Pierce, and J. L. Wesley, *Polym. Commun.*, **24**, 130 (1983).
(30) G. Capaccio, A. G. Gibson, and I. M. Ward, ref 2, p 12.
(31) See ref 1, Chapter 7.
(32) W. G. Perkins, N. J. Capiati, and R. S. Porter, *Polym. Sci. Eng.*, **16**, 200 (1976).
(33) P. Smith, P. J. Lemstra, and J. P. L. Pijpers, *J. Polym. Sci., Polym. Phys. Ed.*, **20**, 2229 (1982).
(34) A. Kelly, "Strong Solids", 2nd ed., Clarendon Press, Oxford, 1973, Chapter 2.

Adsorption of Polyacrylamide on Solid Surfaces. Kinetics of the Establishment of Adsorption Equilibrium

E. Pefferkorn, A. Carroy, and R. Varoqui*

Centre de Recherches sur les Macromolécules (CNRS), 67083 Strasbourg Cedex, France.
Received March 13, 1985

ABSTRACT: The kinetics of the establishment of adsorption equilibria of polyacrylamide onto chemically modified glass beads was studied by a radioactive tracer method using ^{3}H-labeled polymers. The adsorption rates were determined as a function of temperature and surface affinity by varying the surface density of the interacting sites. The experimental conditions were chosen to minimize diffusion effects. Quantitative analysis shows that adsorption is governed by the structure of the surface layer; in particular, the adsorption rate is proportional to the number of free interacting surface sites. The role of the diffuse polymer layer as a barrier rate-limiting factor is also discussed.

Introduction

In previous work we measured the rate of exchange of adsorbed ^{3}H-labeled polymers with nonlabeled polymers in the bulk and analyzed the adsorption rates in the region of adsorption equilibrium.[1] In this paper, we discuss the factors involved in the establishment of adsorption equilibrium.

A study of the rate of establishment of adsorption equilibrium of polymers at solid/liquid interfaces is of fundamental importance in many areas (polymer processing, flocculation of colloidal particles, adhesion, coating, etc.) From a conceptual point of view, the adsorption of polymers implies rate-controlling factors that are not encountered with ordinary molecules. In particular, because of their chainlike structure, the adsorbed surface films of polymers are structurally similar to the surface of a gel, and the rate of adsorption depends not only on the mechanism of adherence to the surface by multiple points of physical adsorption but also on the rate of penetration of a gellike layer. Adsorption rates of polymers have been studied in the past.[2] However, the most interesting features were often blurred by trivial ones (for example, mass transfer by diffusion of polymers to the surface, which depends heavily on the hydrodynamic conditions, presents no interest on its own). Furthermore, the experimental conditions were frequently such that equilibrium was rapidly established in a few minutes or even a few seconds[3,4] and, owing to experimental difficulties, the kinetic parameters could not be assessed with certainty.

In this study of the adsorption of polyacrylamide in aqueous solution on the surface of modified silica particles, the experimental conditions were chosen to ensure a certain number of meaningful points: (i) the nature and density of the surface sites interacting with the polymer were characterized quantitatively, and one objective was to correlate the adsorption kinetics with the "active" site density; (ii) experimental conditions were chosen to minimize bulk diffusion effects (very often, adsorption was carried out in a semiinfinite and unstirred medium by transferring adsorbent plates into a vessel containing the polymer solution); (iii) a very sensitive determination of adsorption was obtained via ^{3}H labeling.

Table I
Characteristics of Glass Beads

sample code	mean diam, μm	spec surface area, $cm^2 \cdot g^{-1}$	% comp [AlOH]/[SiOH]
AS0	34	780	0
AS1	34	780	5
AS2	34	780	12

Experimental Section

1. Polymer. Radioactive polyacrylamide was prepared by radical polymerization in the presence of traces of acrolein. After fractionation, the resulting material was reacted in aqueous solution with tritiated potassium borohydride to yield the following chemical structure (details are given in ref 1):

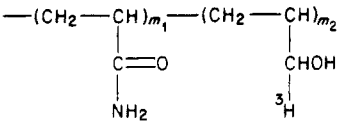

$m_1/m_2 = 10^3$

The characteristics of the sample used in this study are as follows: $M_w = 1.2 \times 10^6$; polydispersity (GPC) = 1.25; specific radioactivity = 1.12×10^8 counts·min^{-1}·g^{-1}.

2. Adsorbents. Nonporous glass beads (Verre et Industrie) of 34-μm average diameter were used as the adsorbent. The surface was first made hydrophilic by soaking for 24 h in hot hydrochloric acid medium

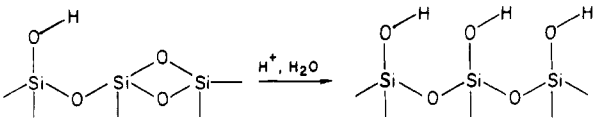

and was then treated with aluminum chloride in chloroform in order to replace some silanols (SiOH) by aluminum chloride

0024-9297/85/2218-2252$01.50/0

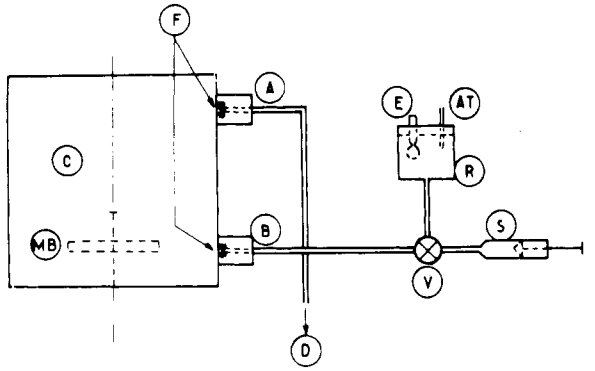

Figure 1. Diagrammatic representation of the experimental device: (C) cell, (A) outlet and (B) inlet of polymer solution, (R) reservoir, (AT) automatic pH titrator, (E) glass and reference electrodes, (F) cellulose acetate filters, (MB) magnetic bar, (S) automatically driven syringe, (V) two-way valve, (D) to fraction collector.

groups, which by hydrolysis of the latter are converted to aluminol (AlOH):

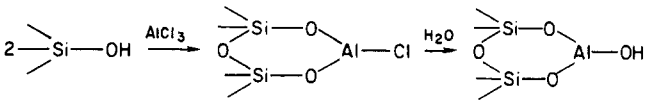

Characteristics are reported in Table I. The [AlOH]/[SiOH] ratio was obtained by assuming 8 SiOH per Å^2 [5] and from the amount of aluminols determined by isotopic exchange of ^{22}Na and ^{23}Na in 5×10^{-5} M NaCl and pH 9 medium.[6]

3. Adsorption Isotherm Determination. An aqueous solution of radioactive polyacrylamide (4 mL) containing a known amount of polymer was transferred into a Perspex cell that contained 45 mL of a carefully degassed suspension of approximately 1 g of chemically modified glass beads in water. Adsorption was allowed to take place under mild and controlled agitation. At different time intervals, the agitation was stopped, allowing the beads to settle, 0.5 mL of the supernatant was quickly sucked through orifice A (Figure 1), and the quantity of polymer adsorbed was calculated by analysis of the radioactivity of the supernatant solution. In all experiments, the radioactivity of the supernatant reached a plateau value in a time interval of <1 h.

4. Adsorption Rate Determination. The adsorption was performed in a manner that enabled the rate of adsorption to be determined with precision as a function of time. To this end, after the cell had been filled with a suspension of 1 g of glass beads, a radioactive polymer solution (0.02 mg/mL) was introduced into the cell at a constant flow rate J_v = 0.5 mL/min via orifice B, by means of an automatically driven syringe included in the flow circuit. The effluent at orifice A was collected by fractions of 0.5 mL (corresponding to time intervals Δt of 1 min), and the radioactivity of all fractions was analyzed. In order to obtain a precise value of the polymer concentration in the effluents, all collected samples were weighed.

The equation describing the conservation of radioactivity in this experiment is

$$SA_s(t) = J_vA_0t - (V - \delta S)A(t) - S\int_0^{\delta} A(x,t)\,dx - J_v\sum_{i=1}^{n} A_i \quad (1)$$

$$n = t/\Delta t \quad (2)$$

S is the total surface, A_0 is the specific activity (counts·mL^{-1}·min^{-1}) of the radioactive polymer solution injected at a constant rate into the cell at orifice B, $A_s(t)$ (counts·cm^{-2}·min^{-1}) and $A(t)$ (counts·mL^{-1}·min^{-1}) are respectively the specific activities of the surface of the glass beads and of the bulk solution in the cell at time t, V is the volume of the cell minus the volume V occupied by the solid (V = 48.6 mL), δ is the thickness of the unstirred layers around each glass bead, $A(x,t)$ is the specific activity in the stagnant layers at position x (it is also assumed that $\delta \ll R$), and subscript i refers to a radioactive sample of volume v = 0.5 mL collected at orifice A at time $i\Delta t$, the symbolism used implying that $A_n(t) = A(t)$.

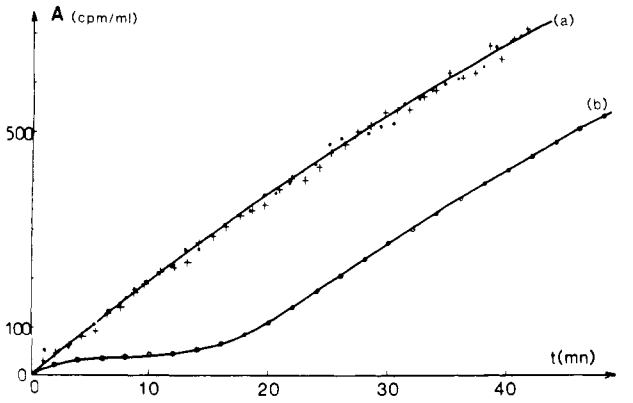

Figure 2. Variation of the radioactivity of the effluent as a function of time. Curve a: (—) calculated from eq 3; (●) activity recorded in the absence of glass beads; (+) activity recorded in the presence of nonadsorbing AS0 glass beads. Curve b is the activity of the effluent in the presence of chemically modified AS2 beads.

In all experiments, the pH was maintained constant by means of an automatic pH titrator (Tacussel). The activity of the effluent corresponding to three different experimental runs is shown in Figure 2.

(i) In the experiment denoted by (●), curve a, a radioactive solution was injected at orifice B in the absence of glass beads (the cell being filled with pure water). The full line in Figure 2, curve a, was computed according to eq 3, which is easily derived from the mass conservation eq 4

$$A = A_0\{1 - \exp[-J_vt/(V + \Delta V)]\} \quad (3)$$

$$(V + \Delta V)\,dA/dt + J_vA = J_vA_0 \quad (4)$$

(ii) In the experiment denoted by (+), the same solution was injected in the presence of nonadsorbing (AlOH free) glass beads (AS0).

(iii) Points denoted by (○), curve b, give the activity of the effluent in the presence of adsorbing glass beads (AS2).

Observing that within experimental precision (≃1%), points (●) and (+) fall on the calculated curve, we infer from eq 1 and 4 that

$$\Delta V_D(\bar{A} - A) \simeq A\Delta V \quad (5)$$

ΔV_D being the volume and $\bar{A}$ the mean activity per unit volume in the stagnant layers. Since the contribution of ΔV in eq 4 is less than 1%, the contribution of the stagnant layers can also be neglected. (From the calculations reported in paragraph 2.2 of the Results, it appears that $\Delta V_D \ll \Delta V$.) With negligible error $A_s(t)$ may therefore be calculated by the following equation:

$$SA_s(t) = J_vA_0t - VA(t) - J_v\sum_{i=1}^{n} A_i \quad (6)$$

In the presence of adsorbing material, the radioactivity in the cell remains at a low level during a time lag of ≃20 min, corresponding to the adsorption period. Equation 4 is recovered after the completion of adsorption and both curves a and b have the same asymptotic time behavior.

The concentration C_s (mg·cm^{-2}) or N_s (mol·cm^{-2}) is proportional to the activity

$$N_s = 0.744 \times 10^{-14}A_s \quad (7)$$

and the mass conservation equation is

$$V\,dN/dt + J_vN + S\,dN_s/dt = J_vN_0 \quad (8)$$

N is expressed in moles, subscripts s and 0 refer respectively to surface quantities and injection concentrations, and N is the concentration in the cell.

Results

1. Adsorption as a Function of pH, Temperature, and Surface Composition. The adsorption isotherms at

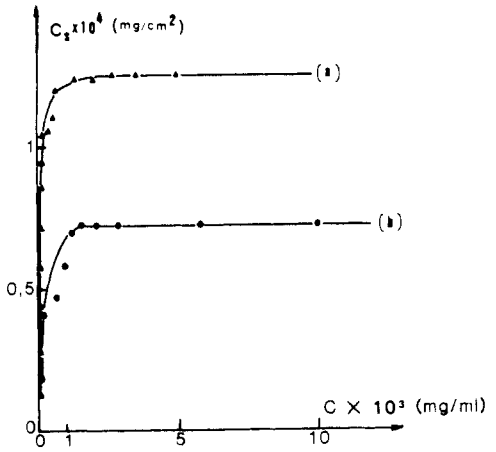

Figure 3. Adsorption isotherms for polyacrylamide adsorbed on AS1 glass beads at $T = 25$ °C: curve a, pH 4.5; curve b, pH 4.0.

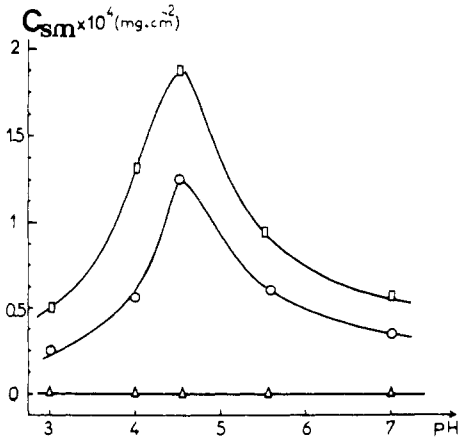

Figure 4. Maximum adsorption as a function of pH and [AlOH]/[SiOH] ratio: (△) nonmodified beads; (○) 5% aluminol grafting; (□) 12% aluminol grafting.

pH 4 and 4.5 for AS1 beads (5% aluminol conversion) are reported in Figure 3. The adsorption reaches a plateau value at extremely low bulk concentrations. It is also pH-dependent. In Figure 4 is shown the adsorption recorded at saturation as a function of the pH and [AlOH]/[SiOH] surface composition. The adsorption presents a maximum at pH 4.5 and increases markedly with the conversion of silanols into aluminols. In the absence of the activating AlOH groups (AS0 sorbent) the adsorption reaches zero. This is in agreement with the observation of Griot and Kitchener, who noted that polyacrylamide does not flocculate aged silica and suggested that amide groups do not interact with hydrogen-bonded silanol groups.[7] Polyacrylamide reacts, however, with AlOH residues. The pH optimum is related to the amphoteric nature of the AlOH residue. From the potentiometric acid–base titration curves, one observes that below pH 4.5 a large fraction of the aluminols are in the $AlOH_2^+$ state, whereas above pH 4.5 the negatively charged AlO^- form is present. Amides and aluminols are able to react at pH 4.5 with one another to form hydrogen bonds.

Figure 5 shows the maximum adsorption on AS1 at pH 4.5 as a function of temperature. The adsorption decreases steadily from 15 to 35 °C. It drops considerably above 35 °C within a short temperature interval to reach low values. Although this behavior is not completely understood, it is probable that competition between intramolecular and surface–polymer hydrogen bonds and breacking of these bonds is at the origin of the unusual temperature behavior. It has been shown that hydrogen bonding between amide

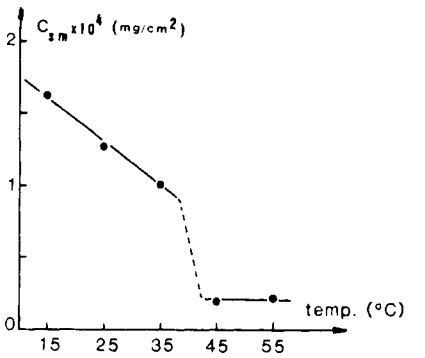

Figure 5. Maximum adsorption as function of temperature at pH 4.5 on AS1 beads.

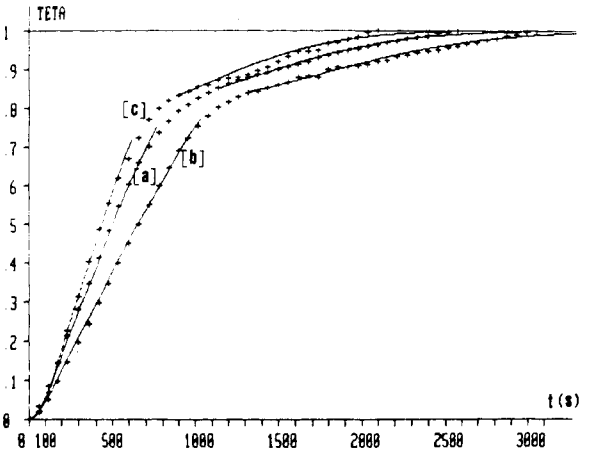

Figure 6. Reduced adsorption as a function of time at 25 °C on AS2 beads: (a) pH 4; (b) pH 4.5; (c) pH 5.5. (—) Continuous lines calculated from eq 12; (+) experimental.

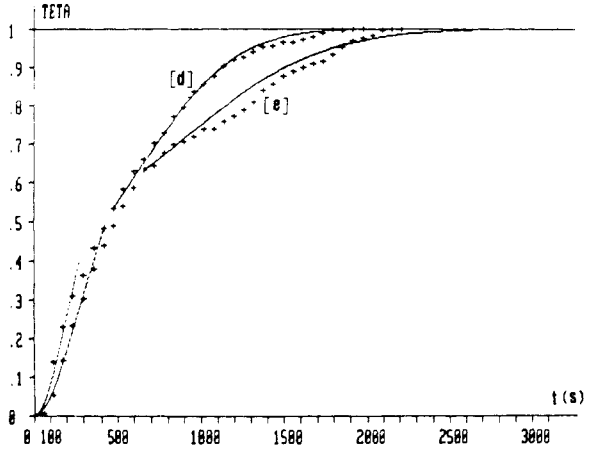

Figure 7. Reduced adsorption as a function of time at 25 °C on AS2 beads: (d) pH 3.0; (e) pH 7.0. (—) Continuous line calculated from eq 12; (+) experimental.

groups in solution compacts somewhat the polyacrylamide conformation.[8]

2. Adsorption Kinetics. The reduced adsorption θ (TETA) = $N_s(t)/N_{sm}$ (N_{sm} being the maximum adsorption) is reported as a function of time in Figures 6 and 7 for different pH values ($T = 25$ °C and AS2 adsorbent). In Figures 8 and 9, θ is represented as a function of time for different temperatures at constant pH (pH 4.5 and AS1 adsorbent). Each kinetic run shows typically two domains. The adsorption increases steeply (almost linearly) up to θ values of about 0.6–0.7, whereas above this value a more then tenfold decrease in the rate is observed and the adsorption reaches very slowly its asymptotic value. The

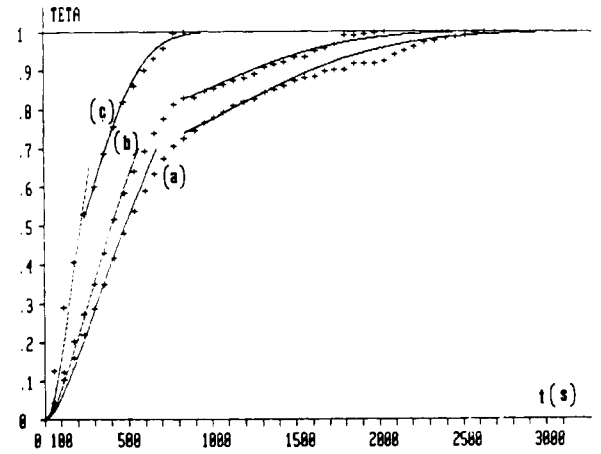

Figure 8. Reduced adsorption as a function of time at pH 4.5 on AS1 beads: (a) 25 °C; (b) 35 °C; (c) 45 °C. (—) Continuous line calculated from eq 12; (+) experimental.

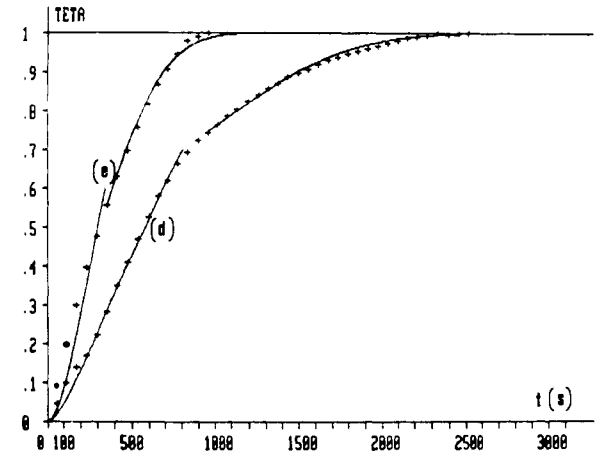

Figure 9. Reduced adsorption as a function of time at pH 4.5 on AS1 beads: (d) 15 °C; (e) 55 °C. (—) Continuous line calculated from eq 12; (+) experimental.

crossover between the two regimes takes place in a narrow θ range.

2.1. Description in Terms of Available Sites. In order to carry out a quantitative analysis of the data we have to examine all possible rate-controlling processes. For the moment, we postpone the examination of diffusion in the stagnant layers around each glass bead, which may slow down the adsorption rate. We shall return later to this point and show that under the experimental conditions diffusion effects can be neglected. At present, we assume that the interfacial resistance to adsorption is chiefly dependent on the structure of the interface at a given time and consider the three possible adsorption mechanisms summarized by the following equations:

$$dN_s/dt = K_1N(t)(1 - \sigma N_s) \quad (9)$$

$$dN_s/dt = K_2N(t)F(N_s) \quad (10)$$

$$dN_s/dt = K_3N(t)(N_{sm} - N_s) \quad (11)$$

In eq 9, σ is the surface area "occupied" by one molecule in the adsorbed state, $N_s(t)$ and $N(t)$ are the concentrations (mol/cm^2 and mol/cm^3, respectively) of polymer in the adsorbed state and in the bulk, and K_1 is a rate constant. The factor $1 - \sigma N_s$ signifies that the adsorption probability, when a molecule comes into the reaction zone, is proportional to the fraction of free surface.[9,10] Distant surface polymers are treated as "hard" particles in analogy to the picture used in the statistical mechanics calculations of the second virial coefficient in dilute polymer solutions.[11]

Table II
Calculated Parameter Values according to Eq 11 at Variable pH

pH (25 °C, AS2)	$N_{sm} \times 10^{13}$, mol/cm^2	$K_D \times 10^{-9}$ [a]	$K \times 10^{-9}$ [a]	$K' \times 10^{-9}$ [a]	K/K'
3.0	0.52	5.5	8.5 (0–0.30)	1.8 (0.55–1.0)	3.0
4.0	1.11	6.0	6.0 (0–0.68)	0.70 (0.85–1.0)	8.6
4.5	1.67	5.5	5.5 (0–0.75)	0.65 (0.84–1.0)	10
5.5	0.74	5.5	5.5 (0–0.65)	0.90 (0.85–1.0)	6.1
7.0	0.511	4.5	4.5 (0–0.40)	0.80 (0.63–1.0)	5.6

[a] In cm^3·mol^{-1}·s^{-1}.

Obviously, this simple idea holds true only in the spirit of Langmuir adsorption in a regime of low surface coverage.[12] We note that, apart from the experiments at 45 and 55 °C, the strong overlapping of molecules that occurs already at low θ values makes the application of eq 9 highly questionable. Indeed, the radius of gyration of the polymer ($M_w = 1.2 \times 10^6$) is 580 Å in aqueous solution,[13] and if adsorption occurs without much conformational change a simple calculation shows that the θ values at which the fraction of free surface becomes zero are $\theta = 0.14$ (pH 4), $\theta = 0.1$ (pH 4.5), and $\theta = 0.2$ (pH 5.5). $\theta = 1$ at pH 4.5 would correspond to approximately ten superposed impermeable molecules.

From polymer–surface studies, it is well-known that not all the polymer sites are actually in contact with the surface and parts of the chain build up a surface layer of molecular dimension. Equation 10 implies that the rate-controlling process originates from the barrier opposed by the surface layer of already-adsorbed polymer (the idea is reminiscent of a diffusion–reptation mechanism for the passage of a long chain through a swollen polymeric gel[17]). In this view, the pertinent parameter is the surface concentration N_s) and the rate would thus be governed by an (unknown) function of N_s. A plot of dN_s/dt vs. N_s did, however, not display a unique representation, irrespective of pH and temperature values. Instead, we found that eq 11 applied reasonably well, provided the two adsorption regimes were characterized by two different constants K and K'.

In eq 11 we assume that the rate is governed by the number of free adsorption sites (if p is the fraction of segments in contact with the surface, $p(N_{sm} - N_s)$ is the fraction of free sites and if p is lumped into K_3, we recover eq 11). In treating our data according to eq 11, we combined the mass conservation eq 8 with eq 11 and obtained a first-order nonlinear differential equation in θ.

$$-V(d/dt) \ln (1 - \theta) - J_v \ln (1 - \theta) + KSN_{sm} = J_vKN_0t, \quad K \equiv K_3 \quad (12)$$

Equation 12 was solved numerically (see Appendix) with $\theta = 0$, $t = 0$ as the boundary condition. The variations of θ as a function of time for different pH and temperature values were calculated according to eq 12 and are represented in Figures 6–9. The K and K' values that provided the best fit are reported, together with their domains of application in Tables II and III.

It is important to emphasize that any desorption is ignored in eq 9–11. The neglect of the reverse fluxes (directed from surface to solution) is justified by a previous experimental study where radioactive labeling enabled us to determine the average "lifetime" of a polymer in the adsorbed state.[1] No desorption was observed when the solution in "equilibrium" with the adsorbent was replaced

Table III
Calculated Parameter Values according to Eq 11 at Variable Temperature[a]

T, °C, (pH 4.5, AS1)	$N_{sm} \times 10^{13}$, mol/cm^2	$K_D \times 10^{-9}$ [b]	$K \times 10^{-9}$ [b]	$K' \times 10^{-9}$ [b]	K/K'
15	1.48	4.0	4.0 (0–0.65)	1.15 (0.75–1.0)	3.5
25	1.17	5.0	5.0 (0–0.50)	0.6 (0.76–1.0)	8.6
35	1.00	7.5	7.5 (0–0.62)	0.85 (0.83–1.0)	8.8
45	0.158	8.0	12 (0–0.45)	5.0 (0.50–1.0)	2.4
55	0.167	4.5	6 (0–0.48)	3.5 (0.55–1.0)	1.7

[a] The supply of modified glass beads AS2 was not sufficient to permit the completion of measurements at different temperatures on the same material. The effect of temperature was measured on AS1 glass beads, which explains the different N_{sm} values at pH 4.5 and 25 °C. [b] In cm^3·mol^{-1}·s^{-1}.

by pure solvent. In the presence of solute molecules, a slow bimolecular exchange, with zero net flux from surface to solution, was observed. However, the rate of exchange was found to be several orders of magnitude less than the adsorption rate, which led us to consider the surface polymer layer to be in a metastable state.

2.2. Diffusion Layer Effects. In varying the rate of stirring, we found no significant modification of the adsorption rates. This observation precludes a diffusion-controlled process. Nevertheless, we considered it necessary to obtain more quantitative information on diffusion effects, and we incorporated diffusion processes in the treatment of eq 11. Assuming a concentration gradient in a stagnant layer around each bead, we must solve eq 10, coupled with Fick's laws

$$\frac{\partial N(x,t)}{\partial t} = D\frac{\partial^2 N(x,t)}{\partial x^2} \qquad 0 \le x \le \delta \tag{13}$$

$$dN_s/dt = K_D N(0,t)(N_{sm} - N_s) \tag{14}$$

Equation 13, in which D is the diffusion coefficient, applies in a region of thickness δ (the unstirred Nernst layer), while the adsorption rate according to eq 11 and 14 is proportional to the solute concentration at $x = 0$.

With the concentration in the diffuse layer expressed as a power series, the system of eq 13 and 14 reduces to a nonlinear differential equation in θ of infinite order. In limiting ourselves to an expansion up to the fifth derivative $[\partial^5 N(x,t)/\partial x^5]_{x=0}$, we obtained a differential equation in θ of the second order (mathematical details are given in the Appendix).

$$A\theta + B\frac{d\theta}{dt} + C\frac{d^2\theta}{dt^2} - \frac{1}{K_D}\ln(1-\theta) - \frac{E}{K_D}\frac{d\ln(1-\theta)}{dt} - F\frac{d^2\ln(1-\theta)}{dt^2} = \frac{N_0 t}{N_{sm}} \tag{15}$$

The constants A, B, C, E, and F, which are all functions of the thickness δ and the known experimental parameters, are reported in the Appendix. Equation 15 was solved numerically with a fourth-order Runge–Kutta method.[18] The fit depends now on the two parameters δ and K_D; fortunately, not much freedom was allowed in the choice of δ and K_D to obtain a reasonable fit. Calculated values are represented in Figures 10 and 11 for $\delta = 5 \times 10^{-5}$ cm (this value gave the best agreement).[19] The K_D values calculated with incorporation of diffusion effects are reported in Tables II and III (third column).

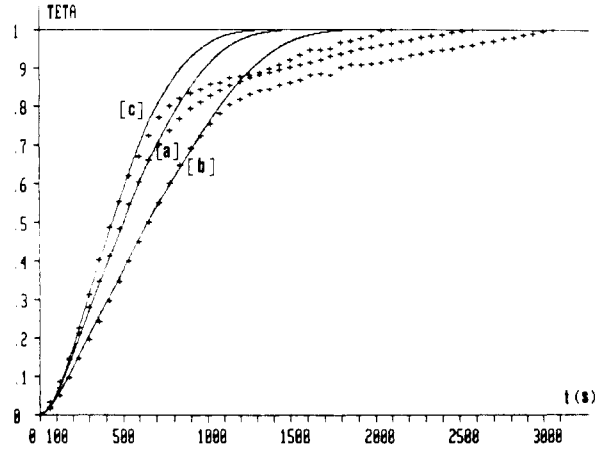

Figure 10. Reduced adsorption as a function of time at 25 °C on AS2 beads: (a) pH 4; (b) pH 4.5; (c) pH 5.5. (—) Continuous line calculated taking into account diffusion effects (eq 15); (+) experimental.

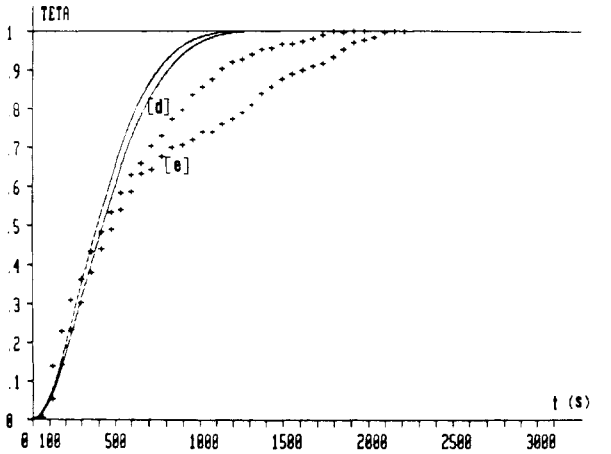

Figure 11. Reduced adsorption as a function of time at 25 °C on AS2 beads: (d) pH 3.0; (e) pH 7.0. (—) Continuous line calculated taking into account diffusion effects (eq 15); (+) experimental.

The calculated diffusion-layer thickness is extremely small (about four molecule diameters), and the K_D values do not depart significantly from those determined by assuming negligible diffusion effects.

Discussion

It was pointed out in paragraph 1 of the Results that adsorption proceeds through hydrogen bond formation between AlOH surface sites and $CONH_2$ polymer groups. From the number of active sites per unit area (this is $8 \times 10^{14}\beta^{-1}$, where β is the [AlOH]/[SiOH] ratio) and from the N_{sm} values (see Tables I and II), one finds a very small average fraction of monomers in "contact" with the surface. The mean $\bar{p}$ value (train monomers over loop monomers ratio) does not exceed 3.0% and 5.7% respectively for AS1 and AS2 sorbents at $T = 25$ °C and pH 4.5. A similar observation was reported for polyacrylamide adsorbed into a porous cellulose acetate filter.[20] The p distribution is however probably not narrow and the stability of some adsorbed macromolecules on the surface might be mainly a consequence of intermolecular hydrogen bonds. That hydrogen bonding actually occurs in concentrated polyacrylamide solutions has been shown by studies of Kulicke and co-workers.[21]

The aluminosilicate surface has no uniform properties on the scale of the monomer dimensions, and the proportionality of the adsorption rate and the number of free sites is in line with expection. The K constant expresses

the kinetic properties of the polymer in the bulk solution. In modeling Brownian motion by a simple jump process, Collins and Kimball have formulated adsorption rates in the presence of a semiadsorbing barrier;[22] the rate of adsorption was found to be $3\alpha DN(t)/l^2$, where l is an average jump length, D the diffusion coefficient, and α the probability of an efficient collision. An extension of the theory to encompasss the adsorption mechanism of large polymer chains would be desirable. According to our results, α should be proportional to the number of available surface sites.

The large change in the rate constant (see column 6 in Tables II and III) above a critical θ_c value is puzzling. It is possible that in order to adsorb polymer in excess of θ_c, some of the attached segments of the previously adsorbed molecules desorb; this would result in large loops and increased film thickness. Such a conformational change in the adsorbed state is expected to be a relatively slow process and, in view of the increased competition for adsorption sites, to occur at high surface coverage. Loop size extension with concentration has been reported for polystyrene adsorbed from cyclohexane onto ferro-type plates;[23] the layer thickness determined by ellipsometry was however found to increase with time in a manner similar to the amount of polymer adsorbed, and the abrupt change reported here is not in line with this observation. For small N_{sm} saturation values, the difference in K and K' is less pronounced, especially at 45 and 55 °C, where the entire curves are almost fitted by unique constants (see Figures 8c and 9e and Table III). Therefore the establishment of the kinetic regime above θ_c is also connected to the appearance of a high segment density at the interface, and an additional resistance opposed by the diffuse layer cannot be excluded. The application of eq 11 does not preclude the mechanism implied by eq 10, insofar as two constants are needed to describe the phenomenology in terms of remaining sites.

Acknowledgment. We are grateful to Dr. G. Chauveteau for several discussions. We acknowledge the financial support of the Institut Français du Pétrole.

Appendix

In order to solve the system of the coupled differential eq 13 and 14, we expand $N(\delta,t)$ in a power series

$$N(\delta,t) = N(0,t) + \delta\left.\frac{\partial N(x,t)}{\partial x}\right|_{x=0} + \frac{\delta^2}{2!}\left.\frac{\partial^2 N(x,t)}{\partial x^2}\right|_{x=0} + \dots \quad \text{(I)}$$

We have, furthermore

$$N(0,t) = -(1/K_D)(d/dt)\ln(1-\theta) \quad \text{(II)}$$

$$\frac{dN_s}{dt} = D\left.\frac{\partial N(x,t)}{\partial x}\right|_{x=0} = N_{sm}\frac{d\theta}{dt} \quad \text{(III)}$$

$$\left.\frac{\partial^2 N(x,t)}{\partial x^2}\right|_{x=0} = \frac{1}{D}\left.\frac{\partial N}{\partial t}\right|_{x=0} = -\frac{1}{DK_D}\frac{d^2}{dt^2}\ln(1-\theta) \quad \text{(IV)}$$

Following this procedure, all partial derivatives can be expressed in terms of derivatives of θ and $\ln(1-\theta)$

$$\left.\frac{\partial^k N(x,t)}{\partial x^k}\right|_{x=0} = -\frac{N_{sm}}{K_D}\frac{d^{l+1}}{dt^{l+1}}\ln(1-\theta), \qquad k = 2l \quad \text{(V)}$$

$$\left.\frac{\partial^k N(x,t)}{\partial x^k}\right|_{x=0} = \frac{N_{sm}}{D^{l+1}}\frac{d^{l+1}}{dt^{l+1}}\theta, \qquad k = 2l+1 \quad \text{(VI)}$$

Substituting eq V and VI in eq I and combining eq I with eq 11 and 8 of the text (retaining up to the fifth derivative in the Taylor expansion) we obtain eq 15 of the text with the following symbols:

$$A = S/J_v + \delta/D$$

$$B = V\delta/J_vD + \delta^3/3!D^2$$

$$C = V\delta^3/3!J_vD^2 + \delta^5/5!D^3 \quad \text{(VII)}$$

$$E = V/J_v + \delta^2/2!D$$

$$F = V\delta^2/2!J_vD + \delta^4/4!D^2 \quad \text{(VIII)}$$

A change of variable enables one to reach a system of two differential equations of first orders

$$y = \ln(1-\theta) \quad \text{(IX)}$$

$$z = dy/dt \quad \text{(X)}$$

$$\frac{dz}{dt} = \left[A - \frac{N_0 t}{N_{sm}} - \frac{y}{K_D} - Ae^y - \left(\frac{E}{K_D} + Be^y\right)z - Ce^y z^2\right]\left(\frac{F}{K_D} + Ce^y\right)^{-1} \quad \text{(XI)}$$

System IX–XI was solved numerically with a Runge–Kutta method of fourth order and the specific boundary conditions

$$y = 0, \qquad z = 0, \qquad t = 0 \quad \text{(XII)}$$

D was taken to be equal to 5.78×10^{-8} cm^2/s in computing the numerical constants defined in eq VII and VIII.[24]

Registry No. Polyacrylamide (homopolymer), 9003-05-8.

References and Notes

(1) Pefferkorn, E.; Carroy, A.; Varoqui, R. *J. Polym. Sci.*, in press.
(2) References on the study of adsorption kinetics are given in: Lipatov, Y.; Sergeeva, L. M. "Adsorption of Polymers"; Wiley: New York, Toronto, 1974; p 17.
(3) Stromberg, R. R.; Kline, G. M. *Mod. Plast.* **1961**, *4*, 20.
(4) Peterson, C.; Kwei, T. K. *J. Phys. Chem.* **1961**, *65*, 1331.
(5) Sears, G. W., Jr. *Anal. Chem.* **1956**, *28*, 1981.
(6) Nabzar, L.; Carroy, A.; Pefferkorn, E. *Soil Sci.*, to be published.
(7) Griot, O.; Kitchener, J. A. *Trans. Faraday Soc.* **1965**, *61*, 1026.
(8) Molyneux, P. In "Water: A Comprehension Treatise"; Franks, F., Ed.; Plenum Press: New York, London, 1975; Vol. 4, p 569.
(9) Varoqui, R.; Pefferkorn, E. *J. Colloid Interface Sci.*, to be published.
(10) Aizenbud, B.; Volterra, V.; Priel, Z. *J. Colloid Interface Sci.* **1985**, *103*, 133.
(11) de Gennes, P.-G. "Scaling Concepts in Polymer Physics"; Cornell University Press: Ithaca, NY, 1979.
(12) Peterson and Kwei (see ref 4) have applied eq 9 to the adsorption of poly(vinyl acetate) from benzene on the surface of chrome plates, with the inclusion of adsorption and desorption fluxes. Their interpretation is obscured by an error arising in the integration of eq 9 (their eq 5 is incorrect). Furthermore the removal of polymers from the surface by pure benzene was found to be negligible, and the postulate of a backard flux is questionable.
(13) Schwartz, L. Thesis, Strasbourg ULP, 1979.
(14) Vincent, B.; Whittington, S. G. In "Surface and Colloid Science"; Matijevic, E., Ed.; Plenum Press: New York, 1982.
(15) Scmitt, A. In "Ecole d'Eté. Colloides et Interfaces. Aussois", Editions de Physique: Les Ulis, France, 1984; p 245.
(16) Fleer, G.J.; Lyklema, J. In "Adsorption from Solution at the Solid/Liquid Interface"; Parfitt, G. D., and Rochester, C. A., Eds.; Academic Press: New York, 1983.
(17) de Gennes, P.-G. *J. Chem. Phys.* **1971**, *55*, 572.
(18) Carnaham, B.; Luther, A. H.; Wilkes, J. O. "Applied Numerical Methods"; Wiley: New York, 1969; p 429.
(19) In ref 1, the analysis of diffusion fluxes was carried out in a different way. As a result of the approximate nature of eq 13 in ref 1, the film thickness was found to be larger than reported here.

(20) Gramain, Ph.; Myard, Ph. *J. Colloid Interface Sci.* **1981**, *84*, 114.
(21) Kulicke, W. M.; Kniewske, R.; Klein, J. *Prog. Polym. Sci.* **1982**, *8*, 373.
(22) Collins, R. C.; Kimball, G. E. *J. Colloid Sci.* **1949**, *4*, 425.
(23) Stromberg, R. R.; Smith, L. E.; McCrackin, F. L. *Symp. Faraday Soc.* **1970**, *4*, 192.
(24) Duval, M. Thesis, Strasbourg ULP, 1982.

Empirical Approach to Phase Equilibrium Behavior of Quasi-Binary Polymer Solutions

Yoshiyuki Einaga,* Zhen Tong, and Hiroshi Fujita

Department of Macromolecular Science, Osaka University, Toyonaka, Osaka 560, Japan.
Received March 18, 1985

ABSTRACT: A simple expression was derived for the Gibbs free energy G of the binary system consisting of monodisperse polystyrene (PS) and cyclohexane (CH) from previously reported light scattering data. By some ad hoc assumptions it was modified to the G function of a system containing two monodisperse PS in CH. No additional parameter was introduced in making this modification. The binodals, cloud-point curves, and critical points calculated with the G function so obtained were found to agree almost quantitatively and consistently with the experimental data of two quasi-binary systems A and B: in A, the polymer is a mixture of PS samples f4 (M_w = 45 300) and f40 (M_w = 498 000), and in B, it is a mixture of PS samples f4 and f10 (M_w = 103 000).

One of the unsolved problems of polymer physical chemistry is the quantitative prediction of phase relationships in macromolecular solutions. Our recent formulation of the Flory–Huggins interaction parameter χ on the basis of light scattering data has made it possible to predict accurately cloud points, spinodal points, and critical points of the binary system consisting of monodisperse polystyrene (PS) and cyclohexane (CH).[1] However, a similar formulation for quasi-binary systems, i.e., solutions containing two or more monodisperse homologous polymers in a pure solvent is considerably more difficult, since a vast amount of light scattering data must be obtained by varying the composition of the polymer mixture as well as the molecular weights of its constituent polymers.

In this paper, we propose another empirical approach to the phase equilibrium behavior of quasi-binary systems. The basic idea is to adapt, by some ad hoc assumptions, the free energy function of a binary system to that of such systems. The assumptions used are tested by comparing their consequences with the experimental data[2,3] previously reported from our laboratory.

Strictly Binary System

Basic Equations. We consider a strictly binary system, made up by dissolving a monodisperse (homo)polymer (component 1) in a pure solvent (component 0). The ratio of the molar volume of component 1, V_1, to that of component 0, V_0, is denoted by P and referred to as the relative chain length of the polymer. As the concentration variable, we adopt a quantity ϕ defined by

$$\phi = n_1V_1/(n_0V_0 + n_1V_1) = n_1P/(n_0 + n_1P) \quad (1)$$

where n_i is the amount in moles of component i and ϕ is the volume fraction of the polymer.

For the reason mentioned below, we formulate the thermodynamic behavior of this system in terms of the difference from that of a hypothetical reference solution in which the chemical potential of the solvent, μ_0^v, is given over the entire range of ϕ by

$$\mu_0^v = \mu_0^\circ - (RT/P)\phi \quad (2)$$

where μ_0° is the chemical potential of the solvent in the pure state and RT has the usual meaning. The chemical potential of component 0, μ_0, in the binary system under consideration may then be represented by

$$\mu_0 = \mu_0^\circ - (RT/P)\phi - \Gamma(T,\phi;P)\phi^2 \quad (3)$$

where $\Gamma(T,\phi;P)$ is an apparent second virial coefficient to be determined by experiment and is related to the Flory–Huggins interaction parameter χ by

$$\Gamma = -\chi - [\ln(1-\phi) + \phi]\phi^{-2} \quad (4)$$

Since Γ is small in poor solvent systems, this relation indicates that χ for such a system contains a large contribution, substantially compensating the second term on the right-hand side ($-[\ln(1-\phi)+\phi]\phi^{-2}$) which is of the order of unity and associated with the entropy of the Flory–Huggins athermal solution. Thus, it does not seem advantageous for the formulation of thermodynamic behavior below the Θ temperature to adopt the traditional χ method in which the Flory–Huggins athermal solution is chosen as the reference state.

The Gibbs–Duhem relation gives

$$[(1-\phi)/V_0](\partial\mu_0/\partial\phi) + (\phi/V_1)(\partial\mu_1/\partial\phi) = 0 \quad (5)$$

where μ_1 is the chemical potential of component 1. Substitution of eq 3 into eq 5, followed by integration, yields

$$\mu_1 = \mu_1^\infty + RT\left[\ln\phi - \phi + \Gamma P\phi(1-\phi) + P\int_0^\phi \Gamma\, du\right] \quad (6)$$

where u is an integration variable and μ_1^∞ is defined by

$$\mu_1^\infty = \lim_{\phi\to 0}(\mu_1 - RT\ln\phi) \quad (7)$$

The G function of the system under consideration is represented by

$$G = n_0\mu_0 + n_1\mu_1 \quad (8)$$

Substitution of eq 3 and 6 gives

$$G = (n_0 + n_1P)\left\{(1-\phi)\mu_0^\circ + \phi\mu_1^\infty P^{-1} + RT\left[-\phi P^{-1} + P^{-1}\phi\ln\phi + \phi\int_0^\phi \Gamma\, du\right]\right\} \quad (9)$$

0024-9297/85/2218-2258$01.50/0